narra j

Original Article

Green algae *Caulerpa racemosa* compounds as antiviral candidates for SARS-CoV-2: In silico study

Asmi CMAR. Tassakka[1]*, Israini W. Iskandar[2], Andi BA. Juniyazaki[3], St Zaenab[4], Jamaluddin F. Alam[1], Haerani Rasyid[3], Kasmiati Kasmiati[1], Ellya Sinurat[5], Fenny M. Dwiany[6], Ronni Martien[7] and Abigail M. Moore[8]

[1]Faculty of Marine Science and Fisheries, Universitas Hasanuddin, Makassar, Indonesia; [2]Postgraduate School of Biomedicine, Universitas Hasanuddin, Makassar, Indonesia; [3]Faculty of Medicine, Universitas Hasanuddin, Makassar, Indonesia; [4]Faculty of Fisheries, Universitas Cokroaminoto, Makassar, Indonesia; [5]Indonesia National Research and Innovation Agency, Jakarta, Indonesia; [6]School of Life Science and Technology, Institute Teknologi Bandung, Bandung, Indonesia; [7]Faculty of Pharmacy, Universitas Gadjah Mada, Yogyakarta, Indonesia; [8]Graduate School, Universitas Hasanuddin, Makassar, Indonesia

*Corresponding author: citra@unhas.ac.id

Abstract

Green algae (*Caulerpa racemosa*) are known to contain bioactive compounds which are hypothesized to have antiviral activities against severe acute respiratory syndrome coronavirus 2 (SARS-CoV-2), the causative agent of coronavirus disease 2019 (COVID-19) pandemic. The aim of this study was to analyze the anti-SARS-CoV-2 potential of compounds extracted from the green alga *Caulerpa racemosa* using in silico analysis. The extract was obtained through maceration with 96% ethanol and the compounds present in the extract were identified through gas chromatography-mass spectroscopy (GC-MS). The binding affinities were analyzed in silico using the PyRx application and visualized in the PyMOL software. GC-MS analysis of *Caulerpa racemosa* extract showed 92 spectral peaks, each of which was assigned to a bioactive compound. Of the six compounds with a strong binding affinity, n-[1-(1-adamantan-1-yl-propyl)-2,5-dioxo-4-trifluoromethyl-imidazo lidin-4-yl] 4-methoxy-benzamide had the lowest score (-8.1 kcal/mol) against the SARS-CoV-2 3C-like protease binding site, similar with that of remdesivir. The molecular dynamics calculations demonstrated that root means square deviation values of the selected inhibitors remained stable throughout a 15-nanosecond simulation. In conclusion, the in silico analysis suggests that *Caulerpa racemosa* extract is a potential antiviral candidate against SARS-CoV-2.

Keywords: Antiviral activity, binding affinity, *Caulerpa racemosa*, SARS-CoV-2, green algae

Introduction

Corona viruses cause immune system dysregulation, leading to respiratory diseases such as severe acute respiratory syndrome (SARS) or Middle East respiratory syndrome (MERS). Caused by severe acute respiratory syndrome coronavirus 2 (SARS-CoV-2), coronavirus disease 2019 (COVID-19) is a disease that can be transmitted through droplets which are expelled when breathing, sneezing, coughing, and speaking, making it highly contagious and easily spread from person to person through everyday human interaction [1,2]. Researchers have studied the therapeutical agents which could attenuate COVID-19, in particular through looking at the potential of herbal medicines [3–5]. These include oils extracted from some plants, such as

https://narraj.org/

Received: May 25, 2023 - Accepted: July 24, 2023 - Published online: July 26, 2023

ginger, guava, and eucalyptus, that are known to contain phytochemical compounds with potential as immunomodulators in the human body [6].

As an archipelagic nation, Indonesia is blessed with abundant marine resources and among these, marine algae or seaweeds are still underutilized. Seaweeds can produce primary and secondary metabolites with a wide range of uses, including applications in the pharmaceutical industry [7]. Previously, seaweed metabolites have been reported to possess antihypertension, antibacterial, antitumor, antioxidant, antifungal, anti-hypercholesterolemia, and antiviral properties, and some seaweeds have been specifically reported as being capable of boosting the immune system [7–9]. Macroalgae have been proposed in prevention and treatment of COVID-19, including *Porphyra umbilicalis*, *Caulerpa racemosa*, and *Gelidium* sp. [10]. Of these, the green seaweed *C. racemosa* is native to South Sulawesi where it is called *lawi-lawi* and tends to be abundant in shallow coastal water [11]. Despite studies on the use of macroalgae in the prevention and treatment of COVID-19 [7–10], the specific therapeutic potential of *C. racemosa* extract, particularly from the South Sulawesi region, against SARS-CoV-2 remains largely unexplored. The aim of this study was to examine the antiviral potential of *C. racemosa* extract through a novel approach by employing molecular docking and molecular dynamics (MD) simulation.

The main principle of molecular docking is the scoring function that can be used to determine the binding mode and position of a ligand, predict binding affinity, and identify potential drugs for a given target protein. The purpose of molecular docking analysis is to quantitatively predict the strength of molecular binding and provide data based on the level of ligand binding affinity to the protein [12]. Several studies have used the docking process in the search for COVID-19 antiviral drugs [13–15]. This study followed the approach used in a previous study [10], analyzing molecular docking using the PyRx application and visualizing it using PyMOL.

Methods

Seaweed sample collection and processing

The *C. racemosa* were obtained from Kayangan Island, Makassar, South Sulawesi Province, Indonesia (119°20.52'E, 5°7.38'N). The freshly harvested samples were placed in containers for transport and further processing. The samples were identified using morphometric techniques and voucher specimens from the samples were stored at the Faculty of Marine Science and Fisheries, Universitas Hasanuddin, Makassar. Before extraction, 11 kg of freshly harvested seaweed was prepared by washing under running water several times until it was free from saltwater precipitate. The seaweed samples were sorted and cleaned while still wet to remove epiphytes and other impurities that may have been collected during the sampling process. The seaweed was then sun-dried for approximately eight hours per day until completely dry. To further prepare the samples for extraction, they were cleaned with distilled water to remove any remaining particles. The cleaned samples (90.8 g) were dried in an herb drier.

Extraction and GC-MS analysis of active compounds in *Caulerpa racemosa*

The dry *C. racemosa* samples macerated for a period of 3 days in 700 ml of 96% ethanol solution, with an ethanol to sample volume ratio of 2:1. The macerated mixture was then filtered through filter paper to obtain a filtrate. The mixture was filtered using a rotary evaporator to obtain the *C. racemosa* extract. Gas chromatography-mass spectroscopy (GC-MS) was performed to identify the active compounds present in the *C. racemosa* extract. An 0.5 mL aliquot of the extract was injected into the GC-MS spectroscope (QP 2010 Shimadzu Ultra, Kyoto, Japan) with a column length of 30 m and a diameter of 0.25 mm. The ion source temperature was set at 200°C, and the interface temperature was set at 280°C. The initial column temperature was set at 70°C for 2 minutes, followed by a ramp-up to 200°C and finally to 280°C. The sample dilution ratio was normalized to ensure that peaks for all compounds present in the extract were detected and displayed in the chromatogram according to the standard. The compounds present in the *C. racemosa* extract were identified utilizing a comprehensive approach involving GC-MS analysis, and referring to a compound library and standards to ensure accurate and reliable identification

of the active compounds. The active compounds in the extract were identified by comparing the mass spectra and retention times of the observed GC-MS peaks with those of known compounds in the library. The retention times of the observed peaks were compared with those of authenticated standards, allowing for further confirmation of the compound identities.

Analysis of ligand-receptor interactions of anti-COVID-19 candidate compounds with molecular docking

The 3CL-protease (protein code 6LU7) was obtained in PDB format from Protein Data Bank (www.uniprot.org) and the necessary docking requirements such as the ligand and protein structure were then prepared. The ligands used in this study were natural active compounds from the *C. racemosa* extract identified through GC-MS. The 3D structures of these compounds and of the control inhibitor remdesivir were obtained by downloading the SDF file format from PubChem (https://pubchem.ncbi.nlm.nih.gov/). Remdesivir was selected as the control inhibitor as suggested by the findings from a previous study [16]. After downloading the SDF files, the active compounds from *C. racemosa* and the control inhibitor were visualized using PyMOL (Version 1.2r3pre, Schrödinger, LLC) by adding hydrogen atoms. The PyMOL visualization results were saved in mol2 format to prepare the docking requirements for the ligand and target protein.

Before conducting the docking process, the approach was validated by performing redocking with the native ligand N3 at the active site. All docking procedures were executed using PyRx 0.8 software [17], by inputting the prepared ligand, SARS-CoV-2 protein, and remdesivir control inhibitor data. The grid of the docking box was set to -11.5, 11.7, 69.2 (x, y, z), and the size of the box was 30 x 30 x 30. This configuration allowed for the accurate positioning of the ligands within the active site. The docking analysis data, including molecular docking results, were then utilized to determine the binding affinity between the ligands and the target protein. To visualize the attachment locations and models/poses on the target protein, the ligand and protein interaction data were displayed and analyzed using PyMOL software and Discovery Studio Visualizer v21.1.0.20298 (Schrödinger, New York, United States) to better understand the interactions between the ligands and the SARS-CoV-2 protein.

Molecular dynamics simulation

Gromacs ver2023.1 (https://www.gromacs.org/) was used to conduct MD simulations on the complex of between SARS-CoV-2 3-chymotrypsin-like main protease (3CLpro) and n-[1-(1-adamantan-1-yl-propyl)-2,5-dioxo-4-trifluoromethyl-imidazolidin-4-yl]4-methoxy-benzamide (ADM); and between 3CLpro and remdesivir complex. The CHARMM36 force field was chosen for the MD simulation, and the transferable intermolecular potential 3 point (TIP3) water model was employed in the MD system. The system's charge was balanced by introducing ions. Before running the MD simulation, the system underwent energy minimization using the steepest descent integrator for 50,000 steps, with a force convergence criterion set at 1000 kcal/mol/nm. Subsequently, each protein-ligand combination was equilibrated using NVT (constant-temperature, constant-volume ensemble) and NPT (constant-temperature, constant-pressure ensemble) within a time frame of 100 picosecond (ps). Temperature and pressure controllers, specifically the Berendsen and Parrinello-Rahman methods, were used to maintain a temperature of 300 Kelvin and a pressure of 1 bar throughout the equilibration process. The MD simulations were run for a total of 50 nanosecond (ns), and the system coordinates were saved every 2 femtoseconds (fs). This 50 ns duration was considered sufficient for achieving a balance between computational time and information. The data obtained from the fluctuation graph indicated a stable equilibration. Various analytical modules included in the GROMACS package were employed to perform structural and conformational analysis on all systems.

ADMET analysis and SARS-CoV-2 drug properties

The compounds were evaluated for the ADME-Tox (absorption, distribution, metabolism, excretion – toxicity). In this study, the ADME-Tlab 2.0 tool (https://admetmesh.scbdd.com/), developed by the Computational Biology and Drug Design (CBDD)Team of the School of Medicine at Zhejiang University, was utilized. This method enabled the analysis of the drug's solubility, absorption, permeability, and metabolites.

The absorption of a drug is influenced by important molecular properties such as lipophilicity and solubility. Therefore, the oral availability of the compounds was predicted Lipinski's rule of five based on several characteristics. This prediction was carried out using the SwissAdme tool available on the Swiss Bioinformatics website (http://www.swissadme.ch/). The characteristics considered include logP (lipophilicity ≤ 5), molecular weight (MW ≤ 500 g/mol), number of hydrogen bond acceptors (HBA ≤ 10), number of hydrogen bond donors (HBD ≤ 5), rotatable bonds (Rbond ≤ 10), and polar surface area (PSA ≤ 140 Å2).

To assess the ability of the compounds as anti-SARS-CoV-2, the Drug Central 2023 online REDIAL portal (https://drugcentral.org/Redial) was used to provide additional information on each of the candidate compounds. In particular, the SARS-CoV-2 cytopathic effect (CPE) assay to measure the ability of a compound to reverse the cytopathic effect induced by the virus in Vero E6 host cells; the spike-ACE2 (angiotensin-converting enzyme type 2) protein-protein interaction (AlphaLISA) assay to measure the ability to disrupt the interaction between the viral spike protein and its human receptor protein (ACE2); and the SARS-CoV-2 3CL biochemical assay to measure the ability to inhibit recombinant 3CL cleavage of a fluorescently labelled peptide substrate [18].

Results

The compounds present in the ethanolic extract of *C. racemosa* were identified using the GC-MS method. The GC-MS chromatogram for *C. racemosa* extract consisted of around 92 spectrum peaks which are presented in **Figure 1**. Details of the compounds and their respective relative abundance are presented in **Table S1**. Out of the 92 active compounds identified, the three *C. racemosa* extract compounds with the highest peak areas (%) were 9,12-octadecadienoic acid(z,z), methyl ester (21.31%); hexadecanoic acid, methyl ester (9.83%); and 1,2-benzenedicarboxylic acid (6.83%). Compounds identified from the GC-MS analysis were then used in the docking analysis to observe the interaction between active compounds from *C. racemosa* and the SARS-CoV-2 target protein.

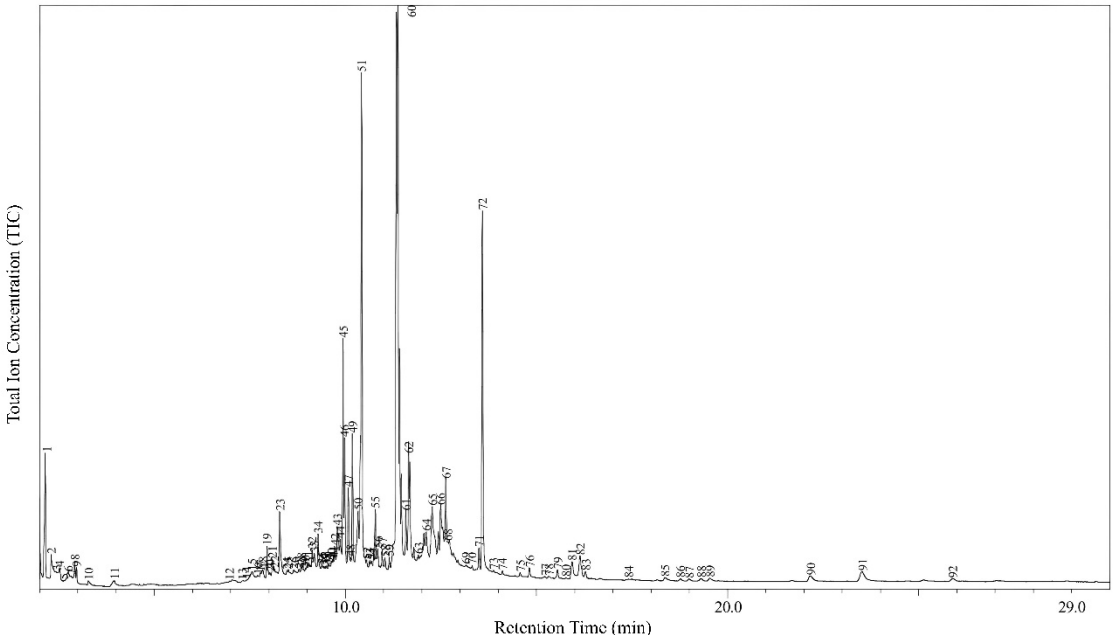

Figure 1. Gas chromatography-mass spectroscopy (GC-MS) spectrophotogram plot of the *Caulerpa racemosa* ethanol extract.

The 3CLpro of SARS-CoV-2 was used as the target protein in the docking process and visualized using the PyMol application. To compare binding affinity, remdesivir as the control inhibitor for the molecular docking process was also visualized in PyMol. Based on the docking analysis, six active compounds contained in *C. racemosa* ethanol extract had binding affinity scores with the SARS-COV-2 which were close to that of remdesivir (-8.1 kcal/mol) (**Table 1**).

Visualization of the interaction between these compounds and the target SARS-CoV-2 protein is presented in **Figure 2**. n-[1-(1-adamantan-1-yl-propyl)-2,5-dioxo-4-trifluoromethyl-imidazo lidin-4-yl]4-methoxy benzamide (abbreviated as ADM) was the compound with the highest binding affinity (-8.1 kcal/mol) and therefore having the highest potential as an antiviral agent.

Table 1. Active compounds contained in the ethanolic extract of *Caulerpa racemosa* and their respective in silico activity against 3CLpro target protein of SARS-CoV-2

Compound	Binding affinity (kcal/mol)	Area (%)
n-[1-(1-Adamantan-1-yl-propyl)-2,5-dioxo-4-trifluoromethyl-imidazolidin -4-yl]4-methoxy-benzamide	-8.1	0.04
Cholesta-4,6-dien-4-ol, benzoate, (3.beta.)-	-7.7	0.07
Lupeol	-7.2	0.15
Stigmasta-5,23-dien-3-ol, (3.beta.)-	-6.8	0.1
Alpha.-Tocopherol-.beta.-D-mannoside	-6.7	0.12
Beta.-Tocopherol	-6.1	0.15
Remdesivir (control)	-8.1	-

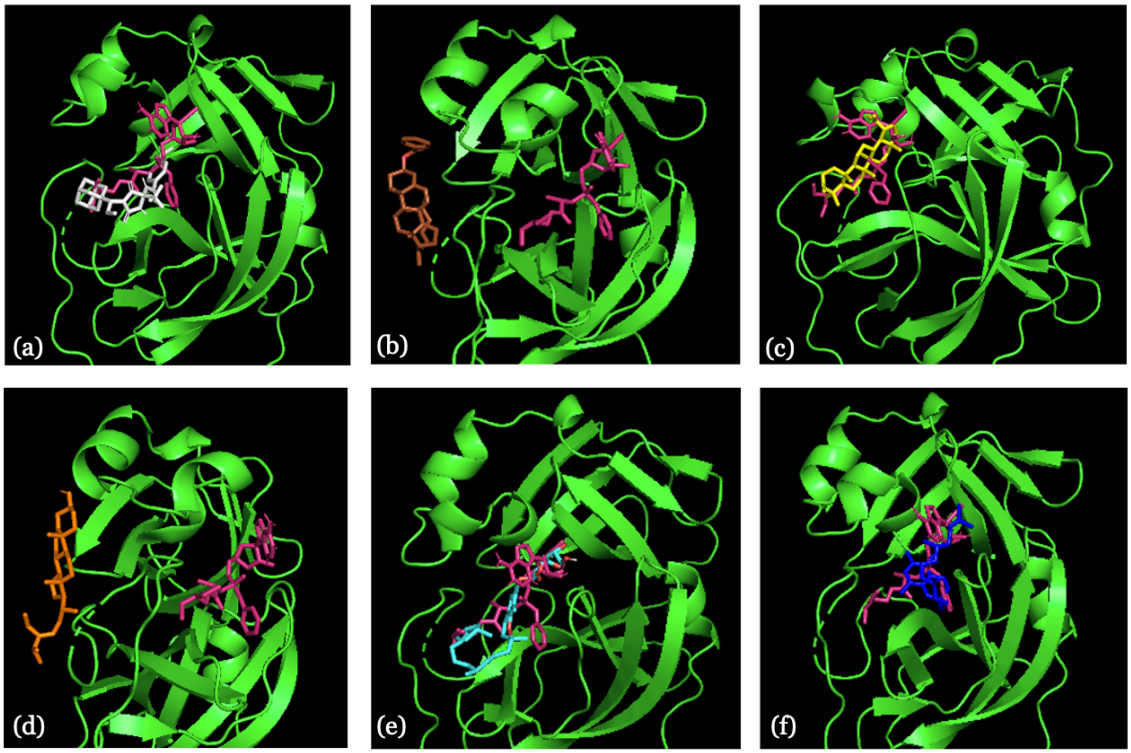

Figure 2. Visualization of ligand interactions between active compounds extracted from *Caulerpa racemosa* by ethanol and the SARS-CoV-2 target protein (3CLpro). (a) n-[1-(1-adamantan-1-yl-propyl)-2,5-dioxo-4-trifluoromethyl-imidazolidin-4-yl]4-methoxy-benzamide; (b) cholesta-4,6-dien-4-ol, benzoate, (3.beta.)-; (c) lupeol; (d) stigmasta-5,23-dien-3-ol, (3.beta.)-; (e) alpha.-tocopherol-.beta.-d-mannoside; (f).beta.-tocopherol; pink: Remdesivir.

To gain a better understanding of the molecular interaction between ADM and remdesivir, a two-dimensional projection of the ligand interaction at active sites is presented in **Figure 3**. The projection shows that the 3CLpro-ADM complex formed five hydrogen bonds with Thr24, Thr45, Ser46, Gly134 and Asn142. Meanwhile, the 3CLpro-remdesivir complex formed three hydrogen bonds, with Leu142, Ser144 and His 164.

Another goal of the in silico study was to employ MD simulations to assess the adaptability of the 3CLpro-ligand complex and the apo system. This was conducted in Gromacs version 2023.1 and factors tracked to assure the simulations' correctness included temperature, pressure, and potential/kinetic energy. To evaluate the rigidity of the complexes, the backbone atom root means square deviation (RMSD) values were determined (**Figure 4a**). The figures showed that apo

3CLpro, 3CLpro-remdesivir complex and 3CLpro-ADM complex attained a stable state after 15 ns. After 45 ns, the systems showed modest changes, but the RMSD values remained largely stable for the rest of the run.

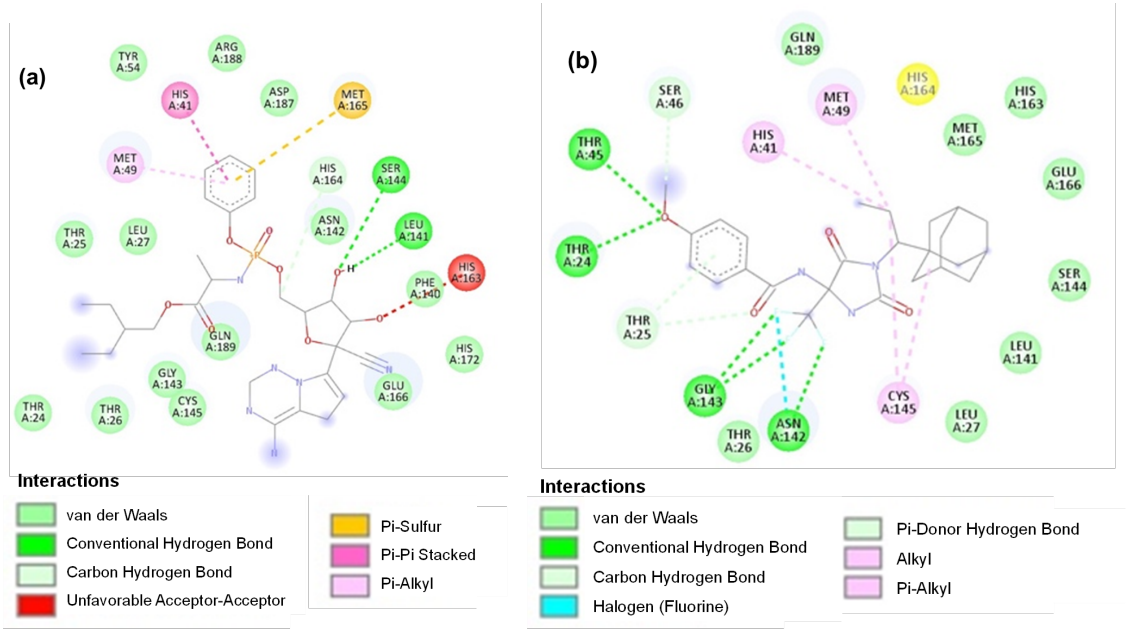

Figure 3. Two-dimensional interactions of (a) 3CLPro-ADM and (b) 3CLPro-remdesivir (control).

To evaluate the flexibility of individual amino acid residues in the targeted protein, the root mean square fluctuations (RMSF) of the backbone atoms were computed for both the apo form and the complex form of 3CLpro-remdesivir and 3CLpro-ADM (**Figure 4b**). Notably, the highest peaks in both systems correspond to specific residues, namely Gln306, Asn51, Pro52, and Asp187, (**Figure 4b**).

The gyrating radius, which is determined by calculating the mass-weighted RMSD of a group of atoms with respect to their shared center of mass, provides insight into the level of protein compaction. By analyzing the trajectory of the radius of gyration (RoG), changes in the overall size of the protein during dynamics can be observed. The RoG values for the apo-3CLpro, the 3CLpro-remdesivir complex, and the 3CLpro-ADM complex (3CLpro-average) were compared and presented in **Figure 4c**. The average RoG for each system was approximately 2.24 nm, indicating a similar level of compaction. Furthermore, the simulation patterns of both systems reached an equilibrium state, as demonstrated by the consistent RoG values throughout the duration of the simulation.

The inhibitor binding affinity for the receptor protein complex, as predicted by the docking simulation studies, was revalidated through the calculation of binding free energy. The estimation was performed for two complexes, 3CLpro-ADM and 3CLpro-remdesivir, using the Molecular Mechanics–Poisson–Boltzmann Surface Area (MM-PBSA) method. The interaction energies (van der Waal's energy, polar solvation energy, electrostatic energy, and overall binding energy), indicated a substantial binding affinity for both compounds with 3CLpro. The computed binding free energy for 3CLpro-ADM and 3CLpro-remdesivir were -26.72 ± 3.40 kcal/mol and 14.32 ± 2.87 kcal/mol, respectively (**Table 2**). However, it is worth noting that 3CLpro-ADM exhibited a higher binding affinity compared to the control compound 3CLpro-remdesivir (**Table 2**). Therefore, the study reaffirmed the strong binding affinity of at least some of these compounds with 3CLpro, with 3CLpro-ADM showing a notably higher affinity than 3CLpro-remdesivir as the control.

Based on ADMET and pharmacokinetic study, some compounds did not fulfill the Lipinski's rule of five (**Table 3**). None of the compounds from C. racemosa extract was predicted to possess the risk of causing acute toxicity or carcinogenicity. In the pharmacokinetics identification, most compounds were acceptable for absorption in digestion tract (**Table 4**).

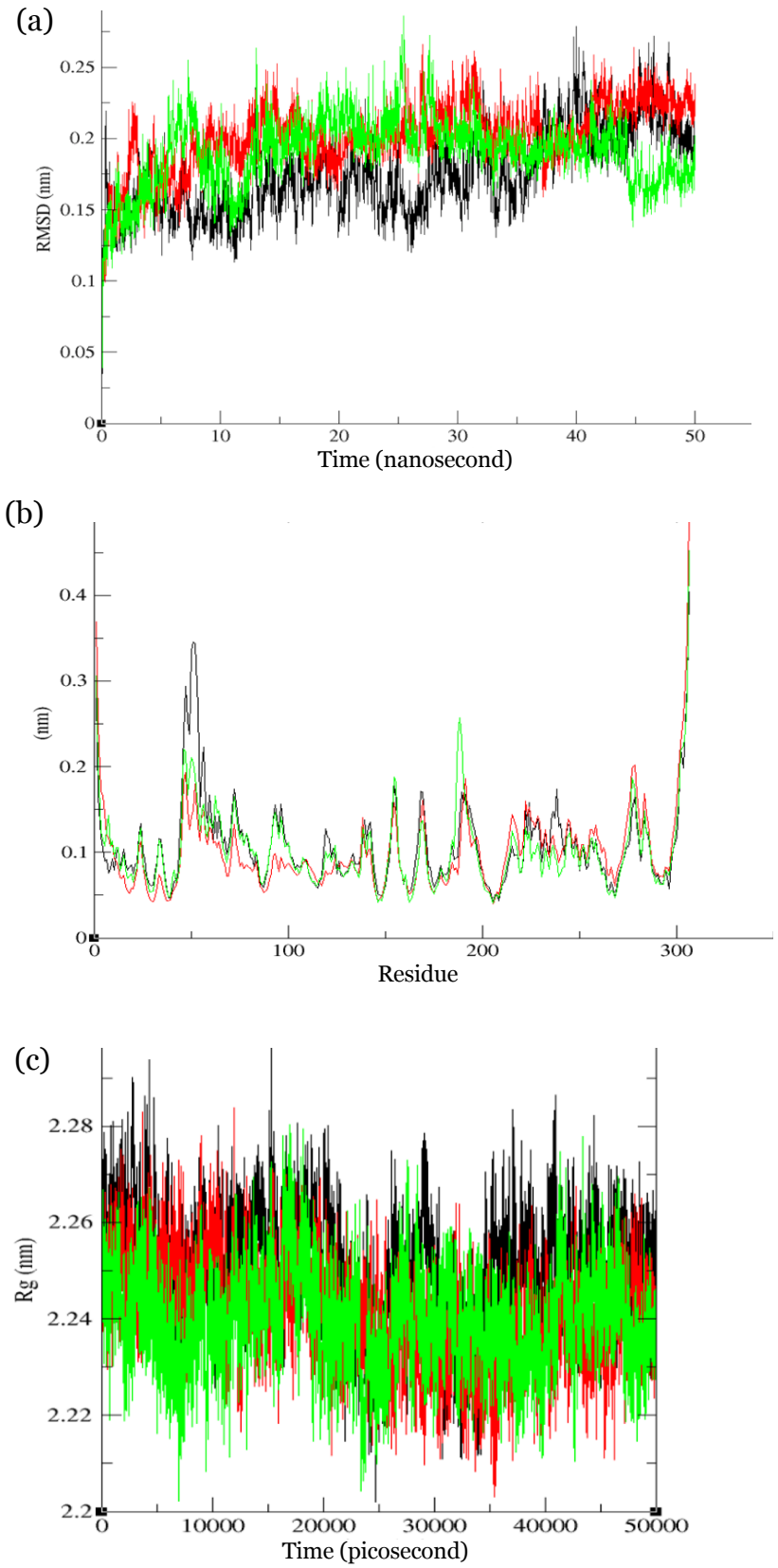

Figure 4. The root means square deviation (RMSD) (a), root mean square fluctuations (RMSF) (b) and radius of gyration (RoG) (c) of 3CLpro-apo (black), 3CLpro-remdesivir complex (red), and 3CLpro-ADM complex (green).

Furthermore, the predicted values of compounds extracted from the green seaweed *C. racemosa* as an anti-SARS-CoV-2 showed promise for drug development (**Table 5**). The

promising anti-SARS-CoV-2 candidates are those that are active for cytopathic effect (CPE); inactive for cytotoxicity; inactive for ACE2; active for 3C-Like enzymatic activity (3CL-EA); and/or active in at least one of the following: AlphaLISA protein-protein interaction, SARS-CoV pseudotyped particle entry counter screen (Cov-PPE), MERS-CoV pseudotyped particle entry (MERS-PPE), and inactive in the counter screen (CS) assays (TruHit, Cov-PPE_CS, MERS-PPE-CS) as well as inactive in human fibroblast toxicity (hCYTOX) (**Table 5**).

Table 2 Binding free energy of 3CLPro-ligand complexes based on MMPBSA calculations (kcal/mol)

Compound	van der Waal's energy	Electrostatic energy	Polar solvation energy	Binding energy
n-[1-(1-Adamantan-1-yl-propyl)-2,5-dioxo-4-trifluoromethyl-imidazolidin-4-yl]4-methoxy-benzamide	-58.11 ±1.74	-24.67 ±1.90	56.05 ±2.22	-26.72 ±3.40
Remdesivir (control)	-38.20 ±0.68	- 9.38±2.55	-33.26 ±1.14	-14.32 ±2.87

Table 3. Lipsinki's rule properties of compounds extracted from *C. racemosa*

Compound	Mass (Da)	Rbond	HBA	HBD	PSA (Å²)	LogP
n-[1-(1-Adamantan-1-Yl-propyl)-2,5-dioxo-4-trifluoromethyl-imidazolidin -4-yl]4-methoxy-benzamide	493	8	7	2	87.74	4.03
Cholesta-4,6-dien-4-ol, benzoate, (3.beta.)-	488	8	2	0	26.30	8.08
Lupeol	462	1	1	1	20.23	7.26
Stigmasta-5,23-dien-3-ol, (3.beta.)-	412	6	1	1	20.23	7.05
Alpha.-Tocopherol-.beta.-D-mannoside	592	16	2	1	108.61	6.59
Beta.-Tocopherol	416	12	2	1	29.45	7.79
Remdesivir (control)	602	14	12	4	213.36	1.50

HBA: number of hydrogen bond acceptor; HBD: number of hydrogen bond donor; logP: PSA: polar surface area; Rbond: rotatable bond.

Discussion

The GC-MS analysis of the *C. racemosa* extract identified a total of 92 active compounds, most of which were fatty acids and alkanes, typically the most prominent phytochemicals in this seaweed (**Table S1**). The profile of bioactive compounds obtained in this present study are similar to those identified previously in the red alga *Halymenia durvillei*, where 37 compounds where identified, most of which were fatty acids [10]. Lipids may act antagonistically to viral infection by direct inhibition or by regulating adaptive and inflammatory responses [19].

The in -silico simulation found that free fatty acids could strongly bind with the spike protein of SARS-CoV-2. The results show that some compounds extracted from *C. racemosa* have lower binding affinity scores compared to remdesivir, except for ADM that has a similar score. Such binding consequently stabilizes the viral spike (S) protein in a locked conformation and reduces its interaction with the ACE2 receptor. This finding has been further confirmed by MD simulation showing complex stability of ADM with 3CLpro. In a previous study, similar fatty acid binding mechanisms have been observed in both SARS-CoV-2 and Middle East respiratory syndrome-related coronavirus (MERS-CoV) [20]. The presence of a competitive bond affinity score for *C. racemosa* extract with the ability to interact *in silico* at the SARS-CoV-2 3CLMpro binding site makes *C. racemosa* extract a potential SARS-CoV-2 antiviral agent candidate.

Table 4. Swiss-ADME prediction of pharmacokinetic properties of compounds extracted from *C. racemosa*

Compound	Gastrointestinal absorption	Blood brain barrier	P-glycoprotein substrate	CYP1A2 inhibitor	CYP2C19 inhibitor	CYP2C9 inhibitor	CYP2D6 inhibitor	CYP3A4 inhibitor
N-[1-(1-Adamantan-1-yl-propyl)-2,5-dioxo-4-trifluoromethyl-imidazolidin -4-yl]4-methoxy-benzamide	High	No	Yes	No	Yes	Yes	Yes	Yes
Cholesta-4,6-dien-4-ol, benzoate, (3.beta.)-	Low	No	No	No	No	No	No	No
Lupeol	Low	No	No	No	No	No	No	No
Stigmasta-5,23-dien-3-ol, (3.beta.)-	Lo	No	No	No	No	No	No	No
Alpha.-Tocopherol-.beta.-D-mannoside	Low	No	No	No	No	No	No	Yes
Beta.-Tocopherol	Low	No	Yes	No	No	No	No	No
Remdesivir (control)	Low	No	Yes	No	No	No	No	Yes

Table 5. Redial predictions of anti-SARS-CoV-2 activity and confidence of compounds extracted from *C. racemosa*

Compound	Live virus infectivity		Viral entry			Viral replication	In vitro infectivity				Human cell toxicity	Host protein
	CPE	CPE-C	α-LISA	TruHit-C	EA	3CL-EA	CoV-PPE	CoV-PPE-CS	MERS-PPE	MERS-PPE-CS	hCYTOX	Sigma1R
N-[1-(1-Adamantan-1-yl-Propyl)-2,5-dioxo-4-trifluoromethyl-imidazolidin -4-yl]4-methoxy-benzamide	Inactive (0.56)	Inactive (0.47)	Active (0.62)	Inactive (0.61)	Inactive (0.69)	Active (0.46)	Active (0.5)	Inactive (0.66)	Inactive (0.53)	Inactive (0.65)	Active (0.58)	Inactive (0.81)
Cholesta-4,6-dien-4-ol, benzoate, (3.beta.)-	Inactive (0.52)	Inactive (0.62)	Active (0.85)	Inactive (0.42)	Inactive (0.82)	Active (0.74)	Inactive (0.52)	Inactive (0.78)	Active (0.73)	Inactive (0.67)	Inactive (0.47)	Inactive (0.76)
Lupeol	Inactive (1.0)	Inactive (1.0)	Active (0.84)	Active (0.8)	Inactive (0.96)	Inactive (1.0)	Inactive (0.55)	Inactive (0.73)	Active (0.66)	Inactive (0.65)	Inactive (1.0)	Inactive (0.85)
Stigmasta-5,23-dien-3-ol, (3.beta.)-	Inactive (0.55)	Inactive (0.9)	Active (0.87)	Active (0.94)	Inactive (0.970	Active (0.7)	Inactive (0.57)	Inactive (0.76)	Active (0.63)	Inactive (0.67)	Inactive (0.86)	Inactive (0.82)
Alpha.-Tocopherol-.beta.-D-mannoside	Inactive (0.88)	Inactive (0.66)	Active (0.78)	Active (0.76)	Inactive (0.67)	Inactive (0.55)	Active (0.7)	Active (0.6)	Active (0.66)	Inactive (0.56)	Active (0.4)	Inactive (0.91)
Beta.-Tocopherol	Active (0.56)	Active (0.58)	Active (0.96)	Active (0.99)	Inactive (0.77)	Active (0.71)	Active (0.58)	Inactive (0.73)	Active (0.55)	Active (0.54)	Active (0.52)	Inactive (0.74)
Remdesivir (control)	Active (1.0)	Inactive (1.0)	Active (1.0)	Inactive (1.0)	Inactive (1.0)	Inactive (1.0)	Active (0.69)	Inactive (0.68)	Active (0.34)	Inactive (0.5)	Active (0.58)	Inactive (0.96)

3CL-EA: 3c-like enzymatic activity; α-LISA: AlphaLISA protein-protein interaction; Cov-PPE: SARS-CoV pseudotyped particle entry; CoV-PPE-CS: SARS-CoV pseudotyped particle entry counter screen; CPE: cytopathic effect; CPE-C: cytopathic effect - cytotoxicity; EA: enzymatic activity; hCYTOX: human fibroblast toxicity; MERS-PPE: MERS-CoV pseudotyped particle entry; MERS-PPE-CS: MERS pseudotyped particle entry counter screen; Sigma1: sigma1 receptor; TruHit-C: TruHit counter protein-protein interaction.

Our hypothesis was supported numerically by the in silico simulation. However, there may be further compounds of other types present in the green alga *C. racemosa* which still need to be identified and analyzed, for example through more advanced molecular approaches. Previous studies also highlight the use of algae in inhibiting the replication of the SARS-CoV-2 [21,22], and compounds or extracts from algae have also been found to be effective against other viruses [23,24]. Following these promising results, some studies under in vitro and in vivo conditions are now needed to further investigate the effectiveness of active compounds from *C. racemosa* in the treatment of COVID-19.

Conclusion

This study investigated the potential of natural compounds derived from *C. racemosa* as antiviral agents against SARS-CoV-2. The findings suggest that the extract from *C. racemosa* holds promise as a candidate for the development of anti-SARS-CoV-2. ADM, one of the compounds, has promising inhibitory effects on the 3CLpro enzyme of SARS-CoV-2 and has the strongest binding affinity. Additional pre-clinical studies, including toxicity testing and in vitro and in vivo investigations are required to fully assess the antiviral potential of *C. racemosa* against SARS-CoV-2.

Ethics approval

Not applicable.

Acknowledgments

The authors acknowledge support from the Indonesian Ministry of Research and Higher Education COVID-19 Research and Innovation Consortium, Fundamental Research scheme, and World Class University (WCU) Program, as well as the Hasanuddin University Laboratories, and the Ujung Pandang State Polytechnic Laboratory.

Competing interests

The authors declare that there is no conflict of interest.

Funding

This research was funded by the Indonesian Ministry of Research and Higher Education under the COVID-19 Research and Innovation Consortium grant No.9/FI/P-KCOVID-19.2B3/IX/2020, the Fundamental Research scheme, and the World Class University (WCU) Program.

Underlying data

The supplementary table can be accessed in https://figshare.com/s/f79472e477ab6d85e318.

How to cite

Tassakka ACMAR, Iskandar IW, Juniyazaki ABA, *et al.* Green algae *Caulerpa racemosa* compounds as antiviral candidates for SARS-CoV-2: In silico study. Narra J 2023; 3 (2): e179 - http://doi.org/10.52225/narra.v3i2.179.

References

1. Wu YC, Chen CS, Chan YJ. The outbreak of COVID-19: An overview. J Chinese Med Assoc 2020; 83:217–220.
2. World Health Organization. WHO Coronavirus (COVID-19) Dashboard 2023.
3. Ang L, Lee HW, Choi JY, *et al.* Herbal medicine and pattern identification for treating COVID-19: A rapid review of guidelines. Integr Med Res 2020; 9:100407.
4. Boozari M, Hosseinzadeh H. Natural products for COVID-19 prevention and treatment regarding to previous coronavirus infections and novel studies. Phyther Res 2021; 35:864–876.

5. Alam S, Sarker MMR, Afrin S, *et al*. Traditional herbal medicines, bioactive metabolites, and plant products against COVID-19: Update on clinical trials and mechanism of actions. Front Pharmacol 2021; 12:1–20.
6. Bhattacharya S, Paul SMN. Efficacy of phytochemicals as immunomodulators in managing COVID-19: A comprehensive view. VirusDisease 2021; 32:435–45.
7. El-Beltagi HS, Mohamed AA, Mohamed HI, *et al*. Phytochemical and potential properties of seaweeds and their recent applications: A review. Mar Drugs 2022; 20:342.
8. Mohy El-Din SM, Mohyeldin MM. Component analysis and antifungal activity of the compounds extracted from four brown seaweeds with different solvents at different seasons. J Ocean Univ China 2018; 17:1178–88.
9. Rosa GP, Tavares WR, Sousa PMC, *et al*. Seaweed secondary metabolites with beneficial health effects: An overview of successes in in vivo studies and clinical trials. Mar Drugs 2020; 18(1):8.
10. Tassakka ACMAR, Sumule O, Massi MN, *et al*. Potential bioactive compounds as SARS-CoV-2 inhibitors from extracts of the marine red alga *Halymenia durvillei* (Rhodophyta) – A computational study. Arab J Chem 2021; 14:103393.
11. Supriadi, Syamsuddin R, Abustang A, Yasir I. Pertumbuhan dan kandungan karotenoid lawi-lawi *Caulerpa racemosa* yang ditumbuhkan pada tipe substrat berbeda. J Rumput Laut Indones 2016; 1:117–122.
12. Ferreira LG, Dos Santos RN, Oliva G, Andricopulo AD. Molecular docking and structure-based drug design strategies. Molecules 2015; 20:13384–421.
13. Chikhale H, Nerkar A. Review on in-silico techniques: An approach to drug discovery. Curr Tre Phar Pharma Chem 2020; 2:24–32.
14. Jin Z, Du X, Xu Y, *et al*. Structure of Mpro from SARS-CoV-2 and discovery of its inhibitors. Nature 2020; 582:289–293.
15. Sampangi-Ramaiah MH, Vishwakarma R, Shaanker RU. Molecular docking analysis of selected natural products from plants for inhibition of SARS-CoV-2 main protease. Curr Sci 2020; 118:1087–1092.
16. Frediansyah A, Nainu F, Dhama K, *et al*. Remdesivir and its antiviral activity against COVID-19: A systematic review. Clin Epidemiol Glob Heal 2021; 9:123–127.
17. Dallakyan S, Olson AJ. Small-molecule library screening by docking with PyRx. Methods Mol Biol 2015; 1263:243–250.
18. KC GB, Bocci G, Verma S, *et al*. A machine learning platform to estimate anti-SARS-CoV-2 activities. Nat Mach Intell 2021; 3:527–535.
19. Schoggins JW, Randall G. Lipids in innate antiviral defense. Cell Host Microbe 2013; 14:379–385.
20. Theken KN, Tang SY, Sengupta S, FitzGerald GA. The roles of lipids in SARS-CoV-2 viral replication and the host immune response. J Lipid Res 2021; 62:100129.
21. Tassakka ACMAR, Iskandar IW, Alam JF, *et al*. Docking studies and molecular dynamics simulations of potential inhibitors from the brown seaweed *Sargassum polycystum* (phaeophyceae) against PLpro of SARS-CoV-2. BioTech 2023; 12:46.
22. Tassakka ACMAR, Sumule O, Massi MN, *et al*. Potential bioactive compounds as SARS-COV-2 inhibitors from extracts of the marine red alga *Halymenia durvillei* (Rhodophyta)-A computational study. Arab J Chem 2021; 14:103393.
23. Permatasari HK, Wewengkang DS, Tertiana NI, *et al*. Anti-cancer properties of *Caulerpa racemosa* by altering expression of Bcl-2, BAX, cleaved caspase 3 and apoptosis in HeLa cancer cell culture. Front Oncol 2022;12:964816.
24. Cirne-Santos CC, de Souza Barros C, Richter CC, *et al*. Inhibition by marine algae of chikungunya virus isolated from patients in a recent disease outbreak in Rio de Janeiro. Front Microbiol 2019; 10:02426.